ASTRONOMY
AND
ASTROPHYSICS

Pick-up ion acceleration at the termination shock and the post-shock pick-up ion energy distribution

S.V. Chalov[1] and H.J. Fahr[2]

[1] Institute for Problems in Mechanics of the Russian Academy of Sciences, Prospect Vernadskogo 101, 117526 Moscow, Russia
(chalov@ipmnet.ru)
[2] Institut für Astrophysik und Extraterrestrische Forschung der Universität Bonn, Auf dem Hügel 71, 53121 Bonn, Germany
(hfahr@astro.uni-bonn.de)

Abstract. It is discussed since quite some time in the literature that the solar wind termination shock may act as an efficient particle accelerator though the underlying physics of injecting particles into this shock acceleration process was not well understood up to now. Most of the earlier work required an ad-hoc prescription of the rate by which particles are injected into the process of diffusive shock acceleration. Here we avoid this injection problem studying instead the single particle fate of pick-up ions arriving at the shock and undergoing multiple adiabatic reflections at the shock. We start out from preaccelerated pick-up ions arriving with a known isotropic distribution function at the shock and suffering reflections or transmissions through the shock depending on their actual velocity space coordinates. Upstream and downstream of the shock the ions in addition are subject to Fermi-2 acceleration processes described by means of a phase-space transport equation for a pitch-angle anisotropic distribution function. As we can show the spectral energy distribution resulting for the downstream pick-up ions consists of two parts, the low energy keV-part which is due to directly transmitted ions and the high energy MeV-part which is due to multiply reflected ions. We also show that the resulting spectrum is fairly sensitive to the location of the shock sector with respect to the upwind direction. This fact is best reflected in corresponding energetic neutral atom (ENA) fluxes reaching the Earth from different directions and thus serves as a unique diagnostic tool for the remote study of the 3-d properties of the termination shock.

Key words: acceleration of particles – shock waves – Sun: solar wind – inteplanetary medium

1. Introduction

What concerns the origin of anomalous cosmic rays (ACRs) it has been shown by Jokipii (1992) that ions in the outer heliosphere can gain energies up to several hundred MeV by diffusive acceleration, however, only at regions where the termination shock is of a quasi-perpendicular nature. But at quasi-

Send offprint requests to: H.J. Fahr

perpendicular shocks the diffusive acceleration process can only operate if velocities of ions to be accelerated are already much higher than the solar wind speed (Jokipii 1987). In order to better physically resolve the injection problem at the termination shock the model of acceleration of pick-up ions by the shock electrostatic potential has been developed (see Lee et al. 1996, Zank et al. 1996b, Zilbersher & Gedalin 1997, Lipatov et al. 1998) in which single particle trajectories in the region close to the shock are calculated. In the model pick-up ions are considered as distributed in velocity space by a shell-like, isotropic distribution function (in the solar wind rest frame) with a velocity radius approximately equal to the solar wind velocity. Those particles out of this distribution with sufficiently small velocities relative to the shock front cannot pass over the electric potential wall and can suffer multiple reflections at this electrostatic cross-shock potential ramp and thereby gain energy till eventually they escape downstream.

Recently Ellison et al. (1999) using a Monte Carlo technique to describe particle trajectories have shown that ACRs can be produced at the termination shock by the diffusive acceleration process originating directly from the pick-up ion population in case their parallel mean free path $\Lambda_\parallel$ near the shock only amounts to a small fraction of an AU (i.e.: the limit of strong scattering). The assumption of such small values of $\Lambda_\parallel$ for pick-up ions near the termination shock, is, however, rather problematic. We meanwhile know that even at 1 AU the parallel mean free path of ions with energies of around 1 keV, at least during some extended periods, can reach values of 1 AU (Gloeckler et al. 1995, Fisk et al. 1997, Möbius et al. 1998, Chalov & Fahr 1999) and strongly increases with the heliocentric distance. This allows to conclude that, in contrast to strong scattering, rather the case of low or moderate pitch-angle scattering near the termination shock appears much more likely. Ion preacceleration processes operating in the heliosphere up to the arrival of the pick-up ions at the termination shock must thus be very important to inject the ions into the shock acceleration process. Pick-up ions preaccelerated by solar wind turbulences have already developed a pronounced high energy tail when they reach the termination shock. A non-negligible fraction of these ions can then experience further acceleration up to energies of

ACRs by means of shock drift and diffusive acceleration (see Chalov & Fahr 1996).

For instance in the paper by Chalov et al. (1997) stochastic preacceleration of pick-up ions by solar wind Alfvénic and magnetosonic turbulences has been considered (in this context see also Isenberg (1987), Bogdan et al. (1991), Chalov et al. (1995), Fichtner et al. (1996), Giacalone et al. (1997), le Roux & Ptuskin (1998)). This approach described the local production of pick-up ions, their convection, adiabatic deceleration and stochastic acceleration in a two-dimensional heliosphere with the symmetry axis oriented along the bulk velocity of the local interstellar medium. As effectively acting solar wind turbulences small-scale Alfvénic fluctuations with correlation lengths of the order of 0.01 AU and large-scale magnetosonic oscillations in the magnitudes of the solar wind velocity and magnetic field with spatial scales of several AU had been considered. The intensities of the fluctuations at 1 AU are described by dimensionless parameters $\zeta_{AE} = \langle \delta B_E^2 \rangle / B_E^2$ and $\zeta_{LE} = \langle \delta U_E^2 \rangle^{1/2} / U_E$ for Alfvénic and large-scale magnetosonic turbulences, respectively. Spectra of accelerated pick-up ions in the region from several AU up to the termination shock have been calculated for appropriate values of the governing parameters.

In this paper we shall take the precalculated spectra in front of the termination shock as initial spectra for the study of a subsequent shock acceleration. As main parameters we shall use again ζ_{AE} and ζ_{LE} in the present approach. More detailed information concerning properties of the turbulent fluctuations including their spatial evolution in the heliosphere can be found in Chalov et al. (1997).

Observations with the ULYSSES spaceprobe (Balogh et al. 1995, Forsyth 1995) have confirmed that the quiet interplanetary magnetic field is close to the Parker spiral field and, therefore, is almost azimuthal in the outer parts of the heliosphere at low and moderate latitudes. If the termination shock had a spherically symmetric shape, then the lines of the interplanetary magnetic field would be nearly perpendicular to the shock normal for the largest part of the shock surface and for the largest part of time, excluded the periods of field polarity changes. In reality due to the interaction of the solar wind with the interstellar medium flow the termination shock has a pronounced upwind-downwind asymmetry (see Baranov & Malama 1993, Pauls & Zank 1996, Fahr et al. 2000). The resulting asymmetry translates into a dependence of the angle, ψ, between the shock normal vector and the upstream Parker magnetic field on the off-axis or longitude angle θ (angle between the solar radian and the interstellar wind axis, see Fig. 1). Quantitatively it follows from calculations carried out by Baranov & Malama (1993, 1995) that ψ varies from $90°$ at the nose of the termination shock to $\approx 65°$ at the flanks. Since the rate of reflection of particles at a shock is very sensitive to the angle ψ (see Kucharek & Scholer 1995), one can expect that the acceleration efficiency of pick-up ions at the termination shock will vary with variation of the angle θ (see Chalov 1993, Chalov & Fahr 1996, Chalov et al. 1997). It is one of the main purposes here to explicitly study this dependence reflected in the resulting postshock pick-up ion spectra. Also
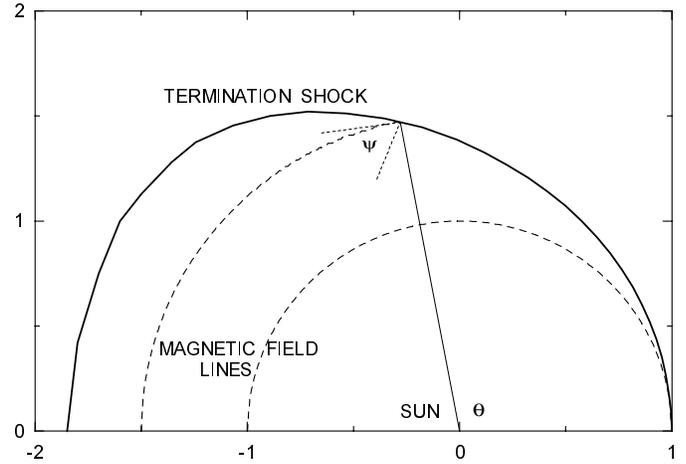

Fig. 1. The shape of the solar wind termination shock in the ecliptic plane as it follows from the twin-shock model by Baranov & Malama (1993). $\theta = 0$ corresponds to the upwind direction.

starting from these spectra we shall calculate fluxes of ENAs which originate at the occasion of pick-up ion dechargings by neutral interstellar H-atoms.

2. Transport and acceleration of pick-up ions near the termination shock

In the present paper the shock drift acceleration of pick-up ions suffering multiple reflections due to experiencing abrupt changes both in the strength and the direction of the magnetic field through the shock is considered. The reflection process operates for high velocity particles different from a simple reflection by the electric cross-shock potential. During the first reflection the mean kinetic energy of pick-up ions increases by approximately a factor of 10 (Chalov & Fahr 1996, Chalov et al. 1997). Reflected particles upstream of the shock have a highly anisotropic velocity distribution. A subsequent exposure of these particles to the turbulent upstream flow causes diffusion in pitch-angle space and, as a result of that, these particles can again return to the shock and thus suffer second or higher order consecutive encounters. In order to describe the motion of particles in the upstream and downstream parts of the solar wind flow in a sufficiently accurate way we here solve the Fokker-Planck transport equation for an anisotropic velocity distribution function.

During a single encounter of charged particles with the shock front we ignore the possible influence of magnetic fluctuations on this process. This seems to be a fairly good approximation in the case when $r_g / \Lambda_\| \ll 1$ which is considered here. It was, however, shown by means of numerical studies (Decker 1988, Kucharek & Scholer 1995) that magnetic fluctuations at quasi-perpendicular shocks can result in some decrease of the reflection efficiency. Cross-field diffusion is not taken into account in our consideration.
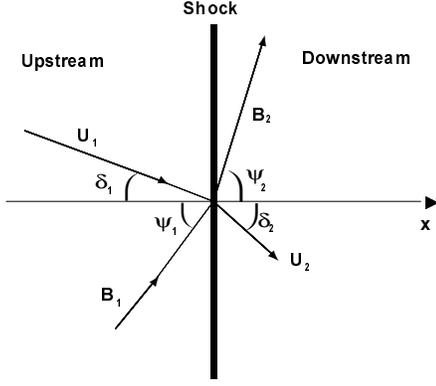
Fig. 2. Schematic illustration of the plasma flow near the termination shock, showing typical pre- and postshock quantities.

2.1. Governing Fokker-Planck equation for anisotropic velocity distribution function

We use here a one-dimensional planar approximation for the plasma flow close to the termination shock. When the x-axis is directed perpendicular to the shock front from the upstream to the downstream part of the flow, then the relevant transport equation to describe the evolution of the gyrotropic velocity distribution function $f = f(t, x, v, \mu)$ of pick-up ions in a background plasma moving at a velocity $\mathbf{U}$ (see Fig. 2) can be written in the following form (Skilling 1971, Isenberg 1997):

$$\frac{\partial f}{\partial t} + (U_x + v\mu\chi)\frac{\partial f}{\partial x} = \hat{S}f + Q(t, x, v, \mu), \qquad (1)$$

where v and $\mu = \cos\xi$ are the velocity and cosine of the particle pitch angle, ξ, in the solar wind rest frame; $\chi = \cos\psi$; ψ is the angle between the shock front and large-scale magnetic field; Q is the local production rate of particles; and $\hat{S}f$ is the scattering operator applied to the function f (see e.g. Schlickeiser 1989):

$$\hat{S}f = \frac{\partial}{\partial\mu}(D_{\mu\mu}\frac{\partial f}{\partial\mu}) + \frac{\partial}{\partial\mu}(D_{\mu v}\frac{\partial f}{\partial v})$$
$$+ \frac{1}{v^2}\frac{\partial}{\partial v}(v^2 D_{\mu v}\frac{\partial f}{\partial\mu}) + \frac{1}{v^2}\frac{\partial}{\partial v}(v^2 D_{vv}\frac{\partial f}{\partial v}). \qquad (2)$$

In Eq. (2) $D_{\mu\mu}$, $D_{\mu v}$, and D_{vv} are the respective Fokker-Planck diffusion coefficients which will be specified below.

In order to solve Eq. (1) numerically it is replaced by an equivalent system of stochastic differential equations (SDEs) describing stochastic trajectories of particles in phase space (for the application of the SDE method to pick-up ion transport and acceleration in the heliosphere see Chalov et al. (1995, 1997), Chalov & Fahr (1996, 1998, 1999), and Fichtner et al. (1996)). To obtain the differential number density of particles, $N = 4\pi v^2 f$, we must simulate a statistically relevant set of stochastic trajectories and determine the density associated with these trajectories in phase space.

2.2. Diffusion coefficients

In order to calculate the Fokker-Planck diffusion coefficients the quasilinear wave-particle interaction theory has been used. Ob-

servations of correlation functions of magnetic fluctuations in the solar wind (see e.g. Matthaeus et al. 1990, Bieber et al. 1996) show that the fluctuations are composed of a combination of a dominant two-dimensional component (wave vectors perpendicular to the mean magnetic field) and a minor slab component (wave vectors parallel and antiparallel to the mean field). Since the two-dimensional component cannot be involved in resonant wave-particle interactions, only the slab component is taken into account here to calculate the diffusion coefficients. In the case of turbulence consisting of nondispersive, nondissipative parallel and antiparallel propagating Alfvén waves the appropriate results have been obtained by Schlickeiser (1989). We only modify his formulas for taking into account dissipation of waves near the ion cyclotron frequency. It is assumed here that the dissipative range has an exponential form, so that the differential intensity of Alfvén waves can be written as (see Bieber et al. 1988, Smith et al. 1990, Schlickeiser et al. 1991)

$$I_\pm^{L,R}(k) = I_{0\pm}^{L,R} k^{-q} \exp(-k l_d) \qquad \text{(for } k > k_{min}\text{)}, \qquad (3)$$

where k is the wavenumber, l_d is the dissipative scale, k_{min} corresponds to the largest scale of energy containing fluctuations, I^L and I^R are the differential intensities of left-hand and right-hand circularly polarized Alfvén waves, respectively, and the signs $(\pm)$ correspond to parallel and antiparallel propagating waves. The mean-squared amplitude of the associated fluctuations is

$$\langle \delta B^2 \rangle = \int_{k_{min}}^\infty (I_+^L + I_-^L + I_+^R + I_-^R)\, dk, \qquad (4)$$

In the following we will assume that left- and right-hand polarized waves have identical intensities. In this case the Fokker-Planck coefficients have the following form (see Chalov & Fahr 1998)

$$D_{\mu\mu} = \frac{U_E}{r_E} D_0 (1 - \mu^2) \left\{ (1 - \mu v_A/v)^2 \times \right.$$
$$\times \mid 1 - \mu v/v_A \mid^{q-1} \exp\left[-\frac{L}{\mid 1 - \mu v/v_A \mid}\right]$$
$$+ \epsilon (1 + \mu v_A/v)^2 \times$$
$$\left. \times \mid 1 + \mu v/v_A \mid^{q-1} \exp\left[-\frac{L}{\mid 1 + \mu v/v_A \mid}\right] \right\}, \qquad (5)$$

$$D_{\mu v} = \frac{U_E v_A}{r_E} D_0 (1 - \mu^2) \left\{ (1 - \mu v_A/v) \times \right.$$
$$\times \mid 1 - \mu v/v_A \mid^{q-1} \exp\left[-\frac{L}{\mid 1 - \mu v/v_A \mid}\right]$$
$$- \epsilon(1 + \mu v_A/v) \times$$
$$\left. \times \mid 1 + \mu v/v_A \mid^{q-1} \exp\left[-\frac{L}{\mid 1 + \mu v/v_A \mid}\right] \right\}, \qquad (6)$$

$$D_{vv} = \frac{U_E v_A^2}{r_E} D_0 (1 - \mu^2) \times$$
$$\times \left\{ \mid 1 - \mu v/v_A \mid^{q-1} \exp\left[-\frac{L}{\mid 1 - \mu v/v_A \mid}\right] \right.$$

$$+ \epsilon \mid 1 + \mu v / v_A \mid^{q-1} \exp\left[-\frac{L}{\mid 1 + \mu v/v_A \mid}\right]\biggr\}. \quad (7)$$

In Eqs. (5)–(7) $\Omega_c = eB/mc$ is the ion gyrofrequency, v_A is the Alfvén speed,

$$L = \frac{\Omega_c l_d}{v_A}, \qquad \epsilon = I_0^- / I_0^+, \quad (8)$$

$$D_0 = \frac{\pi}{4} \frac{\Omega_c r_E}{U_E} \left(\frac{v_A k_{min}}{\Omega_c}\right)^{q-1}$$
$$\times \frac{1}{(1+\epsilon) E_q(l_d k_{min})} \frac{\langle \delta B^2 \rangle}{B^2}, \quad (9)$$

where $E_q(z)$ is the exponential integral

$$E_q(z) = \int_1^\infty y^{-q} \exp(-zy)\, dy. \quad (10)$$

The parameter ϵ is related to the cross helicity h_c of Alfvénic turbulence as $h_c = (1-\epsilon)/(1+\epsilon)$.

2.3. Modelling of pick-up ion reflection at the termination shock

Since in the solar wind rest frame the gyroradius of a typical pick-up ion is much larger than that of a solar wind proton and since the thickness of the shock front can be expected to be of the order of a few gyroradii of solar wind protons, one therefore, for the passage of preaccelerated pick-up ions, can approximate the shock by a discontinuity, neglecting the magnetic field overshot and cross-shock potential in the transition region of the collisionless shock. In this case the reflection conditions at the shock front can be derived from the conservation of the energy of a particle in the de Hoffmann-Teller frame (HT-frame) and from the assumption that the magnetic moment of this particle is the same before and after the encounter with the shock front, i.e. behaves as an adiabatic invariant (Webb et al. 1983). The last assumption is likely to be true for nearly perpendicular shocks but numerical investigations have even shown that this assumption is fairly good also for quasi-perpendicular cases (Terasawa 1979). Recently Meziane et al. (1999) have presented an evidence for acceleration of ions to MeV energies by a single adiabatic reflection at the quasi-perpendicular Earth's bow shock during a CIR (Corotating Interaction Region) event.

The pitch-angle cosines in the upstream plasma frame corresponding to the loss cone in the HT-frame can be written in the form (Decker 1988):

$$\mu_\pm = \varepsilon_1 b^{-1} \pm \left[(1 - b^{-1})(1 - b^{-1}\varepsilon_1^2)\right]^{1/2}, \quad (11)$$

where

$$\varepsilon_i = (U_i/v_i) \sec \psi_i \cos \delta_i, \quad (12)$$

$$b = B_2/B_1. \quad (13)$$

Here ψ_i and δ_i are the angles between the shock normal and the magnetic field vector $\mathbf{B}_i$ on the one hand, and the shock normal

and the solar wind velocity vector $\mathbf{U}_i$, on the other hand (see Fig. 2); v_i is the velocity of pick-up ions in the solar wind frame ($i = 1, 2$ corresponds to the upstream and downstream parts of the flow, respectively). We shall adopt in the following that $\psi_1 + \delta_1 = \pi/2$, excluding thus the polar regions, i.e. magnetic field lines are perpendicular to the solar wind velocity.

Following Decker (1988) one can conclude that:

1) a particle with the pitch cosine μ_1 and velocity v_1 in the upstream flow frame is reflected at the shock if

$$-\varepsilon_1 < \mu_1 \leq \mu_+ \qquad (\varepsilon_1 < 1), \quad (14)$$

$$\mu_- < \mu_1 \leq \mu_+ \qquad (1 \leq \varepsilon_1 < b^{1/2}). \quad (15)$$

In the nonrelativistic case the kinetic energy and the pitch angle of the particle after reflection are given by

$$E_1^R = E_1 \left[1 + 4\varepsilon_1 (\varepsilon_1 + \mu_1)\right], \quad (16)$$

$$\mu_1^R = -(2\varepsilon_1 + \mu_1) \left[1 + 4\varepsilon_1 (\varepsilon_1 + \mu_1)\right]^{-1/2}. \quad (17)$$

2) a particle is transmitted downstream if

$$\mu_+ < \mu_1 \leq 1 \qquad (\varepsilon_1 < 1), \quad (18)$$

$$-1 \leq \mu_1 \leq \mu_- \text{ and } \mu_+ < \mu_1 \leq 1 \quad (1 \leq \varepsilon_1 < b^{1/2}), \quad (19)$$

$$-1 \leq \mu_1 \leq 1 \qquad (\varepsilon_1 \geq b^{1/2}). \quad (20)$$

In this case

$$E_2^D = E_1 \biggl\{ 1 + 2\varepsilon_1 \biggl[\left(1 + b^2/\sigma^2\right) \varepsilon_1/2 + \mu_1$$
$$- (b/\sigma) \left[(\varepsilon_1 + \mu_1)^2 - (b - 1)\left(1 - \mu_1^2\right)\right]^{1/2} \biggr] \biggr\}, \quad (21)$$

$$\mu_2^D = \biggl\{ \left[(\varepsilon_1 + \mu_1)^2 - (b-1)\left(1 - \mu_1^2\right)\right]^{1/2} - b\varepsilon_1/\sigma \biggr\} \times$$
$$\times \biggl\{ \left[b\varepsilon_1/\sigma - \left[(\varepsilon_1 + \mu_1)^2 - (b-1)\left(1 - \mu_1^2\right)\right]^{1/2} \right]^2$$
$$+ b\left(1 - \mu_1^2\right) \biggr\}^{-1/2}, \quad (22)$$

where $\sigma = U_{x1}/U_{x2}$ is the compression ratio at the shock.

3) a particle is transmitted upstream if

$$-1 \leq \mu_2 < -\varepsilon_2 \qquad (\varepsilon_2 < 1). \quad (23)$$

In this case

$$E_1^U = E_2 \biggl\{ 1 + 2\varepsilon_2 \biggl[\left(1 + \sigma^2/b^2\right) \varepsilon_2/2 - \mu_2 -$$
$$(\sigma/b) \left[(\varepsilon_2 + \mu_2)^2 + \left(1 - b^{-1}\right)\left(1 - \mu_2^2\right)\right]^{1/2} \biggr] \biggr\}, \quad (24)$$

$$\mu_1^U = \left\{ -\left[(\varepsilon_2 + \mu_2)^2 + (1 - b^{-1})(1 - \mu_2^2) \right]^{1/2} + \sigma \varepsilon_2/b \right\}$$
$$\times \left\{ \left[\sigma \varepsilon_2/b + \left[(\varepsilon_2 + \mu_2)^2 + (1 - b^{-1})(1 - \mu_2^2) \right]^{1/2} \right]^2 \right.$$
$$\left. + b^{-1}(1 - \mu_2^2) \right\}^{-1/2} . \tag{25}$$

4) an upstream particle does not interact with the shock if

$$-1 \le \mu_1 \le -\varepsilon_1 \qquad (\varepsilon_1 < 1). \tag{26}$$

5) a downstream particle does not interact with the shock if

$$-\varepsilon_2 \le \mu_2 \le 1 . \tag{27}$$

To model the interaction of pick-up ions with the termination shock we have used the following procedure: When pick-up ions, preaccelerated by the stochastic acceleration mechanism in the whole region from the Sun up to the termination shock, arrive at the termination shock their local velocities, i.e. the actual magnitudes v of their velocities in the solar wind rest frame are therefore known from foregoing independent calculations. Since the velocity distribution of the particles at their first arrival is considered to be isotropic, the associated pitch angles of these particles can be selected as a set of pseudo-random numbers from a uniform distribution. After that, equipped with the velocity space coordinates of a particle, by means of Eqs. (14), (15), (18)–(20), and (26) we can conclude whether the particle will be reflected or transmitted downstream and calculate its new velocity and pitch angle after interaction with the shock by means of Eqs. (16), (17), (21), and (22). Then by making use of the SDE system the stochastic trajectory of the particle in the upstream or downstream parts of the flow is calculated till either the particle returns to the shock or reaches the upstream or downstream free escape boundaries. In the first case we again use Eqs. (14), (15), (18)–(20), and (26) for particles approaching from the upstream side, and Eqs. (23), (27) for the opposite case. Each calculation stops when the particle reaches one of the free escape boundaries. By a statistically relevant sample of stochastic trajectories we finally obtain the number density of particles in phase space.

2.4. Parameters of the problem

In our study of the particle-shock interaction we consider the compression ratio σ at the shock as a fixed parameter instead of the gasdynamical Mach number. For quasi-perpendicular parts of the termination shock with $U_1 \gg v_{A1}$ one can obtain the following jump conditions from the Rankine-Hugoniot relations:

$$b = B_2/B_1 \approx \sigma \sin \psi_1 , \tag{28}$$

$$v_{A2}/v_{A1} \approx \sigma^{1/2} \sin \psi_1 , \tag{29}$$

$$\tan \psi_2 / \tan \psi_1 \approx \sigma , \tag{30}$$

$$\tan \delta_2 / \tan \delta_1 \approx \sigma , \tag{31}$$

$$U_1/U_2 \approx \sigma \left[\frac{1 + \cot^2 \psi_1}{1 + \sigma^2 \cot^2 \psi_1} \right]^{1/2} . \tag{32}$$

We remind the reader that the case $\psi_1 + \delta_1 = \pi/2$ is considered here.

We also need some additional relations connecting upstream and downstream values of $\langle \delta B^2 \rangle$ and $\epsilon = \langle (\delta B^-)^2 \rangle / \langle (\delta B^+)^2 \rangle$. The relations can be derived from the paper by McKenzie & Westphal (1969) considering transmission of Alfvén waves through shocks. Assuming that forward and backward downstream waves are incoherent (Ko 1998) one can obtain for a fast quasi-perpendicular shock with $U_1 \gg v_{A1}$ that

$$\langle (\delta B_2^+)^2 \rangle = \frac{\sigma(1 + \sigma^{1/2})^2}{4} \langle (\delta B_1^+)^2 \rangle$$
$$+ \frac{\sigma(1 - \sigma^{1/2})^2}{4} \langle (\delta B_1^-)^2 \rangle , \tag{33}$$

and

$$\langle (\delta B_2^-)^2 \rangle = \frac{\sigma(1 - \sigma^{1/2})^2}{4} \langle (\delta B_1^+)^2 \rangle$$
$$+ \frac{\sigma(1 + \sigma^{1/2})^2}{4} \langle (\delta B_1^-)^2 \rangle . \tag{34}$$

From Eqs. (33) and (34) one can easily find that

$$\langle \delta B_2^2 \rangle / \langle \delta B_1^2 \rangle = \sigma(1 + \sigma)/2, \tag{35}$$

$$\epsilon_2 = \frac{(1 - \sigma^{1/2})^2 + (1 + \sigma^{1/2})^2 \epsilon_1}{(1 + \sigma^{1/2})^2 + (1 - \sigma^{1/2})^2 \epsilon_1}. \tag{36}$$

One can deduce from Eq. (36) that if upstream forward and backward waves have the same intensity ($\epsilon_1 = 1$) then intensities of downstream forward and backward waves will also be equal.

In order to calculate the diffusion coefficient D_0 we should evaluate parameters in the right-hand side of Eq. (9). Assuming that the large-scale interplanetary magnetic field has the standard Parker spiral configuration and adopting an electron number density according to $n_e = n_{eE}(U_E/U(r))(r_E/r)^2$ up to the termination shock we obtain for the part of the heliosphere close to the ecliptic plane

$$\frac{v_{A1}}{v_{AE}} = \left[\frac{(r_E/r_{sh})^2 + \omega^2}{1 + \omega^2} \frac{U_1}{U_E} \right]^{1/2} , \tag{37}$$

where $\omega = r_E \Omega / U_1$ ($\Omega = 2.7 \cdot 10^{-6} \text{s}^{-1}$) and r_{sh} is the heliocentric distance to the termination shock. Here we take into account the deceleration of the solar wind in the outer heliosphere due to charge exchange of solar wind protons with interstellar neutrals. In the following we shall specify pick-up ions as pick-up protons. The ratio v_{A1}/Ω_{c1} for protons can be written as

$$v_{A1}/\Omega_{c1} = 2.3 \cdot 10^7 (n_{e1}/1\text{cm}^{-3})^{-1/2}\text{cm} . \tag{38}$$

The calculations presented here were carried out using the following values for the basic parameters: $U_E = 450 \text{ km s}^{-1}$,

$v_{AE} = 45 \, \mathrm{km \, s^{-1}}$, $n_{eE} = 7 \, \mathrm{cm^{-3}}$, $q = 5/3$, $r_{sh} = 90$ AU, $\epsilon_1 = 1 \, (= \langle (\delta B_1^-)^2 \rangle / \langle (\delta B_1^+)^2 \rangle)$, $\sigma = 3 \, (= U_{x1}/U_{x2})$, $k_{min} = 10^{-11} \, \mathrm{cm^{-1}}$. For measurements of the last value in the inner heliosphere see Belcher & Davis (1971), Jokipii & Coleman (1968). Our knowledge on the value of k_{min} in the outer heliosphere is rather bad (see, however, Zank et al. 1996a). The value of σ and the rate of deceleration of the solar wind in the outer heliosphere (about 15% for $n_{HLISM} = 0.14 \, \mathrm{cm^{-3}}$) were taken from calculations by Baranov & Malama (1993, 1995). What concerns the value of the dissipative scale, we assume here that $l_d = v_A/\Omega_c$ (e.g. $l_{d1} = 0.7 \cdot 10^9$ cm). Finally it can be shown from Eq. (10) that at $z \ll 1$

$$E_q(z) = \frac{1}{q-1} + O(z^{q-1}) \,. \tag{39}$$

The upstream angle ψ_1 between the shock normal and magnetic field lines, and the level of Alfvénic turbulence $\zeta_{A1} = \langle \delta B_1^2 \rangle / B_1^2$ we keep as free parameters.

3. Numerical results for pick-up ions downstream of the shock

In our calculations the inner and outer free escape boundaries were placed at 5 AU from the shock in upstream and downstream direction. The source term in Eq. (1) has the following form:

$$Q(x,v) = Q_0(v)\delta[x - (-0)] \,, \tag{40}$$

where $\delta(x)$ is the Dirac delta function. Thus Eq. (40) means that particles are injected just in front of the shock. The function $Q_0(v)$ corresponds to spectra of pick-up ions accelerated by second-order Fermi processes in the whole region from the Sun up to the termination shock (see Introduction and the end of Sect. 2.3). We do not consider here pick-up ions created in the region downstream of the shock. These ions just after their creation in the rest frame of the subsonic solar wind have a local velocity which is small compared to the thermal velocity of the shocked, downstream solar wind protons. Thus they cannot be considered as a suprathermal component and they have inferior chances to be accelerated to higher energies compared to pick-up ions from upstream regions.

Figs. 3 and 4 show trajectories of three selected particles in configuration and velocity space, respectively, calculated on the basis of the SDE system and of the shock reflection and transmission conditions (14)–(27). All the selected particles start in front of the shock with identical velocities $v_1 = 2U_1$ but with different values of the pitch angle μ_1. The shock normal angle is $\psi_1 = 70°$ and the level of Alfvénic turbulence is taken as $\zeta_{A1} = 0.01$. The space coordinate, particle velocity in the solar wind frame, and time are measured in units of r_E, of U_E, and of r_E/U_E, respectively. The shock is located at $x = 0$. It can be seen from Fig. 3 that one of the particles (solid line) suffers multiple reflections at the shock and moves far upstream. After each reflection the velocity of the particle increases (Fig. 4) while during intervals between consecutive reflections it is approximately constant. It means that stochastic acceleration is not efficient at the adopted level of turbulence and time scales
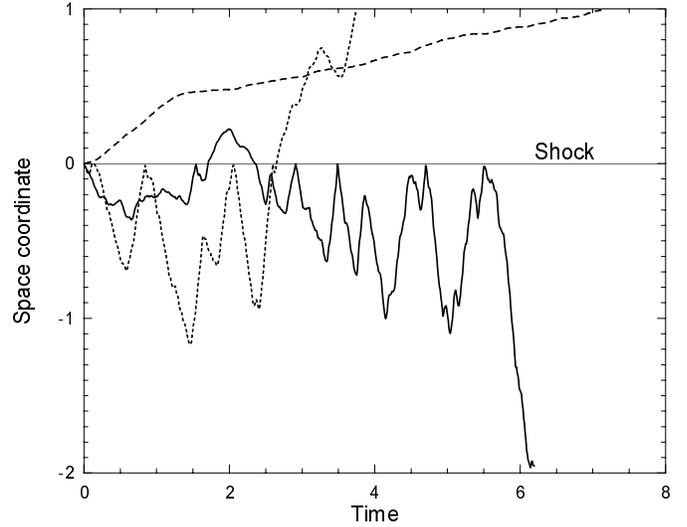

Fig. 3. Trajectories of three particles in configuration space. All the particles start in front of the shock with identical velocities $v_1 = 2U_1$ but with different values of the pitch-angle. The shock normal angle $\psi_1 = 70°$, the level of Alfvénic turbulence $\zeta_{A1} = 0.01$.
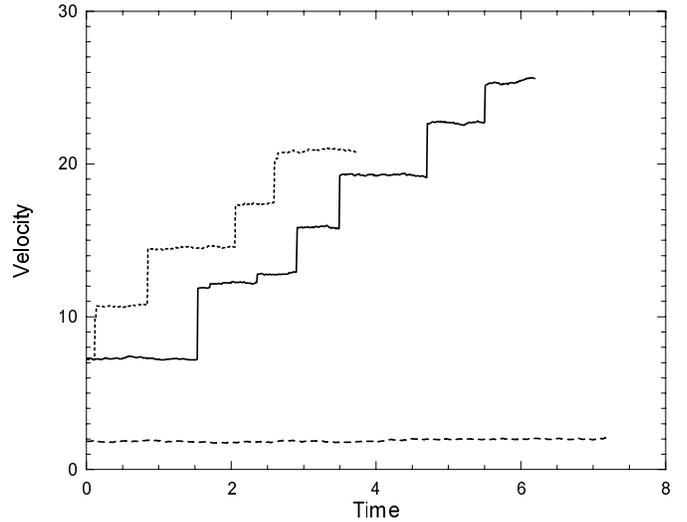

Fig. 4. Same as Fig. 3 but in velocity space.

which are shown. The second particle (dotted line) also suffers multiple reflections but it leaves the shock in a shorter time scale than the first one and as a result its final velocity is lower. Finally the third particle (dashed line) due to its specific initial μ-value has been transmitted through the shock without reflections.

Fig. 5 shows spectral fluxes of pick-up ions in the downstream region of the solar wind at 2 AU from the shock. Calculations of the pitch-angle distribution of pick-up ions show that the velocity distribution function in the solar wind frame has already become almost isotropic at such distances. All fluxes presented in the paper are in the solar wind rest frame but, since we are primarily interested in high energy particles here, their fluxes will be approximately the same in the solar rest frame. In Fig. 5 curve 4 is the initial flux of pick-up ions in front of the termination shock calculated for $\zeta_{AE} = 0.2$ and $\zeta_{LE} = 0.5$
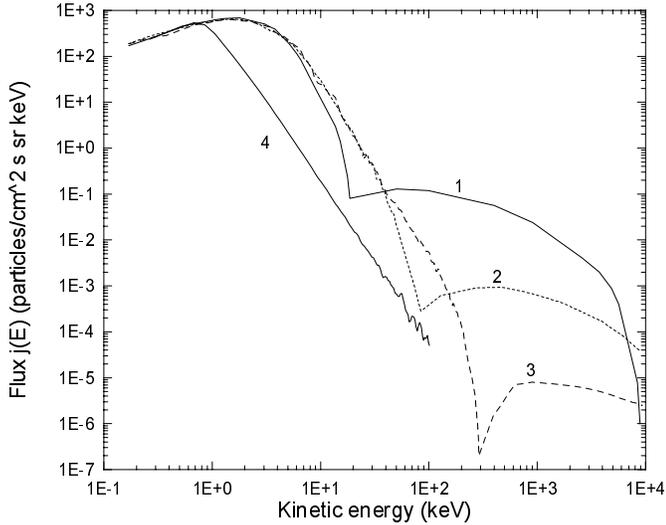
Fig. 5. Downstream fluxes of pick-up ions for different shock normal angles: $1 - \psi_1 = 70°$, $2 - 80°$, $3 - 85°$; $\zeta_{A1} = 0.01$. Curve 4 is the initial flux of pick-up ions in front of the termination shock calculated for $\zeta_{AE} = 0.2$ and $\zeta_{LE} = 0.5$.

Fig. 6. Same as Fig. 5 but $\zeta_{A1} = 0.01$ (solid curves) and $\zeta_{A1} = 0.09$ (dashed curves).

(see Introduction). Curves 1, 2, and 3 are the downstream fluxes in cases when $\psi_1 = 70°, 80°$, and $85°$, respectively, and when $\zeta_{A1} = 0.01$. In the ecliptic plane such shock normal angles correspond to longitudes counted from the upwind direction (see Fig. 1) of $\theta = 80°, 40°$, and $20°$, respectively (see Chalov et al. 1997).

The first outstanding feature which can be recognized in the curves of Fig. 5 is their nonmonotonic spectral slopes. Each spectrum can be considered as consisting of two parts separated by some valley. The low energy parts of the spectra are due to particles which were immediately transmitted through the shock, i.e. which did not suffer multiple reflections. In contrast particles which suffered multiple reflections at the shock constitute the high energy tails.

The second interesting feature emanates from the pronounced dependence of fluxes of high energy particles on the upstream shock normal angle ψ_1. As obvious from our calculations in the region downstream of the shock one can expect considerably higher spectral fluxes of pick-up ions with energies between about 100 keV and several MeV near the flanks of the termination shock as compared to the nose region. At higher energies, however, the fluxes at the nose exceed those at the flanks. Such reaction of the fluxes is connected with two facts: On the one hand, one should notice that, even though the reflection efficiency decreases when the shock normal angle increases, the maximum energy which ions can reach due to reflection nevertheless increases (see Chalov & Fahr 1996). On the other hand, one has to be aware that reflected ions can reach the upstream free escape boundary more easily when ψ_1 is smaller (in the case of the real non-planar termination shock ions reflected at a less oblique portion of the shock penetrate more deeply into the inner parts of the heliosphere than ions reflected at a more oblique one and thus suffer more intensive adiabatic cooling).
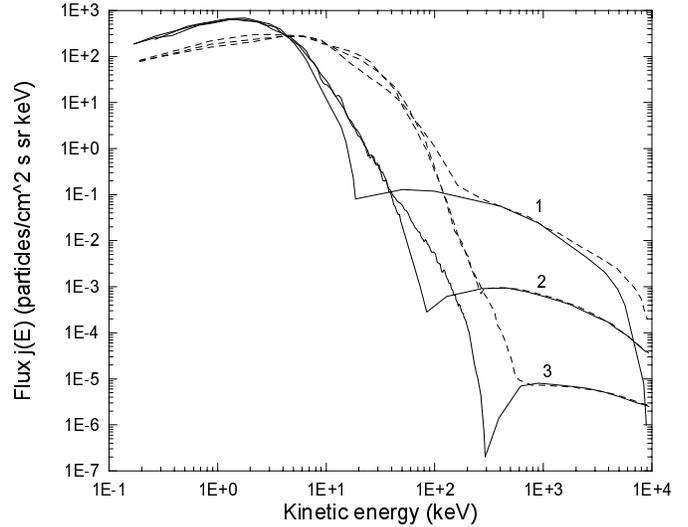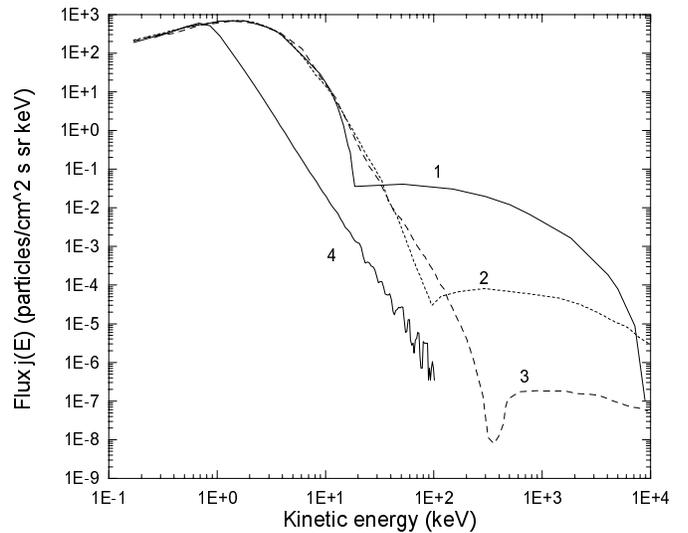

Fig. 7. Same as Fig. 5 but $\zeta_{LE} = 0.3$.

Thus the nose portion of the termination shock is a more effective accelerator of pick-up ions to highest energies ($E \geq 10$ MeV) as generally believed up to now. Strictly speaking the planar geometry is a fairly good approximation only for particles with low and intermediate energies, and it is a rather problematic assumption for high energy ions ($E \geq 10$ MeV) since shock curvature effects can become very important at such energies.

In Fig. 6 the solid curves are the same spectral downstream fluxes as in Fig. 5, while the dashed curves are the downstream fluxes corresponding to a higher level of Alfvénic turbulence characterized by $\zeta_{A1} = 0.09$. First of all one can see that enhanced turbulence results in more efficient stochastic acceleration of the bulk of pick-up ions while the high energy tails of the fluxes are almost identical in both cases. The difference between the tail distributions in the case $\psi_1 = 70°$ (solid and

dashed curves 1) is connected with the fact that high level turbulence prevents energetic ions from upstream escape.

Fig. 7 shows spectral fluxes of pick-up ions downstream of the shock at $\zeta_{A1} = 0.01$ but for different initial pick-up ion upstream flux which had been calculated now adopting the same level of Alfvénic turbulence at 1 AU as in the case presented in Fig. 5, namely $\zeta_{AE} = 0.2$, but reduced amplitude of large-scale oscillations, $\zeta_{LE} = 0.3$. The decrease of preacceleration efficiency throughout the heliosphere results in a considerable reduction of spectral fluxes downstream of the shock at high energies.

The results of this paper presented above should perhaps be compared with results obtained already earlier for postshock pick-up ions along different theoretical approaches like those by Fahr & Lay (2000) on one hand and those by Dworsky & Fahr (2000) on the other hand. In Fahr & Lay (2000) it was assumed that preaccelerated pick-up ions with the same pitch-angle-isotropic initial spectrum as adopted here are convected over the upwind portion of the termination shock assuming a negligible probability of a reflection at the shock. The latter assumption is naturally justified in that case since the upwind shock is of a perpendicular shock type with a tilt of the shock normal of $\psi_1 = 90°$ with respect to the upwind magnetic field. Under these conditions upstream pick-up ions pass over the shock, without any reflections occurring, and their magnetic moment is adopted to be conserved. Simply with Liouville's theorem then the new postshock spectral distribution, however, assumed to be again isotropic in pitch angle μ, is easily obtained. It is interesting to see that in fact the postshock spectrum obtained under these prerequisites is identical to the low energy part of the spectrum obtained in our calculations here, if applied for the case $\psi_1 = 90°$. The second part, the high energy part of the spectrum found in this paper here which is due to pick-up ions having undergone consecutive reflections at the shock is, however, absent in the results by Fahr & Lay (2000) and, as evident, also is not appearing in our present approach under conditions of a perpendicular shock ($\psi_1 = 90°$) where no reflections take place.

On the other hand, in the approach by Dworsky & Fahr (2000) the full transport equation for energetic ions with a pitch-angle-isotropic distribution function including the spatial diffusion term has been solved. As evident this approach addresses the case of strong turbulences operating on the pitch-angle redistribution of the pick-up ions, i.e. is dedicated to the case of the strong scattering limit with $\Lambda_\parallel \simeq r_g$, whereas here our approach just treats the opposite case with $\Lambda_\parallel \gg r_g$. As evident from our figures in this paper in the latter approach for weak scattering both parts of the ion spectrum, low and high energy parts, are separated by a pronounced valley. In the strong scattering limit as shown in Dworsky & Fahr (2000) this valley does not appear anymore as pronounced spectral structure, but low and high energy parts of the spectrum are smoothly connected with eachother. The high energy pick-up ions do appear in both cases, in the first case due to multiple reflections at the shock, in the latter case due to diffusive acceleration, i.e. by Fermi-1 acceleration suffered by particles spatially diffusing backwards

from the downstream into the upstream region. This may tell us that careful treatment of the reflection of anisotropically distributed pick-up ions as described in this paper here more or less leads to similar results concerning the high energy part of the spectrum as spatial diffusion of isotropically distributed energetic pick-up ions. The difference mainly appears in the occurrence of a spectral depletion region (valley) in the first case ($\Lambda_\parallel \gg r_g$) which disappears for the case $\Lambda_\parallel \simeq r_g$. Both cases may in fact be realized during the course of the solar activity cycle; at solar minimum with low turbulence levels one may rather find the spectral depletion feature shown in this paper here, at solar maximum conditions due to enhanced turbulence levels (maybe with some typical delay period, see e.g. Scherer et al. 1998) the spectrum shown by Dworsky & Fahr (2000) may appear as the more typical or the more likely one.

4. Postshock energetic neutral hydrogen atoms (H-ENAs)

The longitudinal dependence of the downstream fluxes of pick-up ions can in principle be checked by remotely sensing or viewing the outer parts of the heliosphere in ENAs. Interesting in this respect are ENAs originating in the region downstream of the shock, i.e. between the termination shock and the heliopause (within the heliosheath). These ENAs are due to charge exchange reactions between downstream pick-up ions and neutral interstellar H-atoms. The resulting flux of H-ENAs at the Earth's orbit in $(\text{cm}^{-2}\,\text{sr}^{-1}\,\text{s}^{-1}\,\text{keV}^{-1})$ is given by (see e.g. Hsieh & Gruntman 1993)

$$j_H(\mathbf{s}, E) = \int_\mathbf{s} j_{pu,H}(\mathbf{r}, E)\sigma(E)n_H(\mathbf{r})\,ds\,, \qquad (41)$$

where $j_{pu,H}(\mathbf{r}, E)$ is the spectral flux of pick-up hydrogen with energy E, $n_H(\mathbf{r})$ is the number density of neutral hydrogen, $\sigma(E)$ is the cross section for charge exchange between pick-up ions and neutral atoms. The integration in Eq. (41) extends from the termination shock to the heliopause along the line of sight with a differential line element ds. The extinction of H-ENAs on the way from the point of creation to an observer at the Earth can be neglected at energies under consideration here.

To estimate the H-ENA fluxes we use a simplified model in which both shape of the heliopause and the plasma sheath flow pattern in between the shock and the heliopause are described by the well known Parker formulas (Parker 1963), while the shape of the termination shock and the hydrogen number density have been taken from calculations by Baranov & Malama (1993, 1995) for the case $n_{H,LISM} = 0.14\,\text{cm}^{-3}$, $n_{e,LISM} = 0.14\,\text{cm}^{-3}$, and $V_{LISM} = 26\,\text{km}\,\text{s}^{-1}$. In order to calculate fluxes of pick-up ions up to the heliopause we simply assume that the velocity distribution function is conserved along the streamlines in the downstream flow. This is a fairly good approximation for the incompressible flow described here (see Parker 1963), since adiabatic cooling and acceleration are not operating. Spatial diffusion and momentum diffusion (or stochastic acceleration) will apparently modify the distribution in some way, however, here we neglect these effects to obtain approximate estimations. The charge exchange cross section
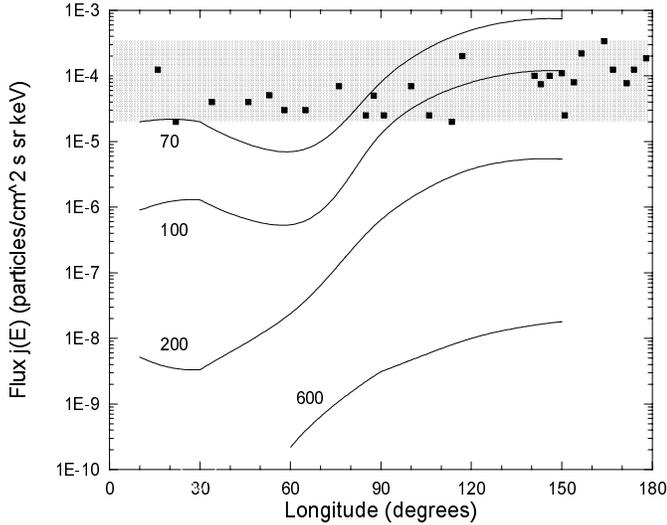
Fig. 8. Fluxes of energetic neutral hydrogen at the orbit of the Earth as functions of longitude, θ, counted from the upwind direction. The numbers denote the energies in KeV. The squares inside the dashed area show differential H-ENA fluxes in the energy range from 55 to 80 keV detected by CELIAS/HSTOF on SOHO (Hilchenbach et al. 1998).

$\sigma(E)$ for high energies needed in Eq. (41) has been taken from Hsieh & Gruntman (1993).

Fig. 8 shows fluxes of H-ENAs with specific energy at the orbit of the Earth (i.e. in the ecliptic plane) as function of longitude, θ, counted from the upwind direction (see Fig. 1). The labels at the curves denote the specific H-ENA energies in KeV. One can see strong longitudinal anisotropies of these fluxes which generally tend to increase toward the downwind direction. Nonmonotonicity of the curves in Fig. 8 is connected with nonmonotonicity of the pick-up ion fluxes. Downwind fluxes ($\theta \cong 180°$) are not shown in Fig. 8 because of the uncertainty of the length of the heliospheric tail (see e.g. Jäger & Fahr 1998). The squares inside the shaded area show differential H-ENA fluxes in the energy range from 55 to 80 keV detected by CELIAS/HSTOF on SOHO (Hilchenbach et al. 1998). In fact the apparent upwind-downwind anisotropy of these fluxes has been observed in the measurements. It is obvious that our simplified model of ENA production in the interface region can display the behaviour obtained from observations only qualitatively. Czechowski & Grzedzielski (1997) also have calculated H-ENA fluxes from the heliosheath originating from decharged ACR protons and also found an increase of these fluxes from the tail region due to increase of the thickness of the heliosheath towards the tail. The initial ACR spectrum at the shock by these latter authors was, however, assumed to be a power law instead of the one which was calculated here. In our present results in addition the longitudinal flux increase over the range from $0°$ to $150°$ is much more pronounced as compared to results given by Czechowski & Grzedzielski (1997) due to the strong longitudinal variation of the downstream pick-up ion fluxes at high energies. This result concerning the pronounced longitude-dependence of H-ENA fluxes is new and very interesting since it could be easily tested by observations. In our calculations here

we did not explicitly look into the effect of varying compression ratios at the shock while this was done in explicit form by Fahr & Lay (2000), however, only for ENA fluxes to be expected from the upwind portion of the termination shock. Putting these results together with those presented here one may easily be convinced that ENA measurements at the orbit of the Earth can be a very good diagnostic tool to study the 3-d structure of the termination shock and of the involved shock physics.

5. Conclusions

Shock drift acceleration of pick-up ions suffering multiple encounters with the termination shock due to pitch-angle scattering upstream and downstream from the shock has been considered in the paper. Stochastic preacceleration of pick-up ions by solar wind turbulences in the whole region from the Sun up to the termination shock has been taken into account. We have shown that in the case of low scattering ($\Lambda_{\|} \gg r_g$) when the velocity distribution function of pick-up ions is anisotropic near the shock front and when the magnetic moment of the ions is the same before and after the encounters with the shock, downstream spectra of the pick-up ions have two interesting features. First of all, the differential fluxes consist of two parts separated by a depletion region. The low energy parts of the fluxes are due to ions which were transmitted through the shock and did not suffer multiple reflections. On the other hand, ions which suffered multiple reflections at the shock constitute the high energy tails. Such nonmonotonic shapes of fluxes are not expected in the case of strong scattering when the diffusive approximation is used. The second feature is the pronounced dependence of fluxes of high energy ions on longitude counted from the upwind direction. The dependence is closely connected with variation of the shock normal angle due to prolate shape of the termination shock. We have calculated differential fluxes of H-ENAs originating in the heliosheath and have found strong upwind-downwind asymmetry of the fluxes both due to the longitudinal dependence of downstream pick-up ion fluxes and increase of the thickness of the heliosheath towards the tail region of the heliosphere.

References

Balogh A., Smith E.J., Tsurutani B.T., et al., 1995, Sci 268, 1007
Baranov V.B., Malama Yu.G., 1993, J. Geophys. Res. 98, 15157
Baranov V.B., Malama Yu.G., 1995, J. Geophys. Res. 100, 14755
Belcher J.W., Davis L., 1971, J. Geophys. Res. 76, 3534

Bieber J.W., Smith C.W., Matthaeus W.H., 1988, ApJ 334, 470
Bieber J.W., Wanner W., Matthaeus W.H., 1996, J. Geophys. Res. 101, 2511
Bogdan T.J., Lee M.A., Schneider P., 1991, J. Geophys. Res. 96, 161
Chalov S.V., 1993, Planet. Space Sci. 41, 133
Chalov S.V., Fahr H.J., 1996, Solar Phys. 168, 389
Chalov S.V., Fahr H.J., 1998, A&A 335, 746
Chalov S.V., Fahr H.J., 1999, Solar Phys. 187, 123
Chalov S.V., Fahr H.J., Izmodenov V., 1995, A&A 304, 609
Chalov S.V., Fahr H.J., Izmodenov V., 1997, A&A 320, 659
Czechowski A., Grzedzielski S., 1997, Adv. Space Res. 19(6), 949
Decker R.B., 1988, Space Sci. Rev. 48, 195
Dworsky A., Fahr H.J., 2000, A&A 353. L1–L4
Ellison D.C., Jones F.C., Baring M.G., 1999, ApJ 512, 403
Fahr H.J., Lay G., 2000, A&A 356, 327
Fahr H.J., Kausch T., Scherer H., 2000, A&A 357, 268
Fichtner H., le Roux J.A., Mall U., Rucinski D., 1996, A&A 314, 650
Fisk L.A., Schwadron N.A., Gloeckler G., 1997, Geophys. Res. Lett. 24, 93
Forsyth R.J., 1995, Space Sci. Rev. 72, 153
Giacalone J., Jokipii J.R., Decker R.B., et al., 1997, ApJ 486, 471
Gloeckler G., Fisk L.A., Schwadron N.A., 1995, Geophys. Res. Lett. 24, 93
Hilchenbach M., Hsieh K.C., Hovestadt D. et al., 1998, ApJ 503, 916
Hsieh K.C., Gruntman M.A., 1993, Adv. Space Res. 13(6), 131
Isenberg P.A., 1987, J. Geophys. Res. 92, 1067
Isenberg P.A., 1997, J. Geophys. Res. 102, 4719
Jäger S., Fahr H.J., 1998, Solar Phys. 178, 193
Jokipii J.R., 1987, ApJ 313, 842
Jokipii J.R., 1992, ApJ 393, L41

Jokipii J.R., Coleman P.J., 1968, J. Geophys. Res. 73, 5495
Ko C.M., 1998, A&A 340, 605
Kucharek H., Sholer M., 1995, J. Geophys. Res. 100, 1745
Lee M.A., Shapiro V.D., Sagdeev R.Z., 1996, J. Geophys. Res. 101, 4777
le Roux J.A., Ptuskin V.S., 1998, J. Geophys. Res. 103, 4799
Lipatov A.S., Zank G.P., Pauls H.L., 1998, J. Geophys. Res. 103, 29679
Matthaeus W.H., Goldstein M.L., Roberts D.A., 1990, J. Geophys. Res. 95, 20673
McKenzie J.F., Westphal K.O., 1969, Planet. Space Sci. 17, 1029
Meziane K., Lin R.P., Parks G.K., et al., 1999, Geophys. Res. Lett. 26, 2925
Möbius E., Rucinski D., Lee M.A., Isenberg P.A., 1998, J. Geophys. Res. 103, 257
Parker E.N., 1963, Interplanetary dynamical process. New York: Interscience
Pauls H.L., Zank G.P., 1996, J. Geophys. Res. 101, 17081
Scherer K., Fichtner H., Fahr H.J., 1998, J. Geophys. Res. 103, 2105
Schlickeiser R., 1989, ApJ 336, 243
Schlickeiser R., Dung R., Jaekel U., 1991, A&A 242, L5
Skilling J., 1971, ApJ 170, 265
Smith C.W., Bieber J.W., Matthaeus W.H., 1990, ApJ 363, 283
Terasawa T., 1979, Planet. Space Sci. 27, 193
Webb G.M., Axford W.I., Terasawa T., 1983, ApJ 270, 537
Zank G.P., Matthaeus W.H., Smith C.W., 1996a, J. Geophys. Res. 101, 17093
Zank G.P., Pauls H.L., Cairns I.H., Webb G.M., 1996b, J. Geophys. Res. 101, 457
Zilbersher D., Gedalin M., 1997, Planet. Space Sci. 45, 693